CIENCIA 12(1), 32 - 44, 2004
Maracaibo, Venezuela

Non-isothermal and isothermal kinetics in commercial 3003 alloys studied by electrical resistivity

Ney J. Luiggi A.

GFM, Departamento de Física, Escuela de Ciencias, Núcleo de Sucre, Universidad de Oriente, Cumaná, Estado Sucre, Venezuela.

Recibido: 10-09-02 Aceptado: 30-03-04

Abstract

Non-isothermal and isothermal transformation kinetics in commercial 3003 alloys were monitored by electrical resistivity ρ using homogenised samples for different heating rates and different ageing temperatures. In the non-isothermal case, as the temperature increases from room temperature to 615°C, ρ decreases to different stages until a minimum value, then grows up to a resistivity value near that of the solid solution, the position and magnitude of the minimum depending on the heating rate. Three different transformation processes are identified. In the isothermal case, which was studied at ageing temperatures between 350°C and 550°C, ρ decreases just up to a plateau, this plateau being more important when the ageing temperature is lower. The isothermal and non-isothermal transformation kinetics were analysed using iso-conversional techniques, obtaining in the isothermal case a decrease of the apparent activation energy between 160 and 80 kJ/mol. The non-isothermal activation energy for the formation of the equilibrium phase at high temperatures was parametrically evaluated, our non-isothermal results for particular values of the N parameter and the transformed fraction being in agreement with energies obtained using the Kissinger relation.

Key words: Electrical resistivity; isothermal; kinetics; non-isothermal; 3003 alloy.

Cinéticas no isotérmicas e isotérmicas en una aleación comercial 3003 estudiadas por resistividad eléctrica

Resumen

Las cinéticas de transformación no isotérmica e isotérmica en una aleación comercial 3003 han sido monitoreadas a diferentes razones de calentamiento y diferentes temperaturas de envejecimiento. En el caso no isotérmico, en la medida que la temperatura es incrementada desde la temperatura ambiente hasta 888 K, la resistividad decrece en diferentes etapas hasta alcanzar un valor mínimo, luego crece hasta un valor de resistividad cercano al valor mostrado cuando los aleantes están en solución sólida, dependiendo la posición y la magnitud del mínimo de la razón de calentamiento. Para este caso se identifican tres diferentes procesos de transformación. son identificados. En el caso isotérmico, el cual fue estudiado para temperaturas de envejecimiento comprendidas entre 623 K y 823 K, decrece hasta alcanzar un plateau, cuya magnitud es más importante en la medida que la temperatura de envejecimiento es mas baja. Ambas cinéticas, las no isotérmicas y las isotérmicas fueron analizadas usando técnicas de iso-

* Autor para la correspondencia. E-mail: nluiggi@sucre.udo.edu.ve

conversión, obteniendo en el caso isotérmico un decrecimiento de la energía aparente de activación entre 160 y 80 kJ/mol. La energía de activación no isotérmica para la formación de la fase de equilibrio a altas temperaturas fue parametricamente evaluada, obteniéndose para determinados valores de N y de la fracción transformada concordancia entre nuestros resultados no-isotérmicos y los obtenidos usando la relación de Kissinger.

Palabras clave: Aliación 3003; isotermico; kinetica; non-isotermico; resistividad eléctrica.

1. Introduction

It is well known that electrical resistivity can be used to obtain information on precipitation and dissolution kinetics in aluminium alloys (1-4). The electrical resistivity reflects the loss of electronic momentum when the electrons are scattered by different scattering centres such as electrons, phonons, impurities, atomic clusters and constituted phases. Adequate thermal treatments dispose the alloy so that the electronic scattering can mainly occur as the result of one of these dispersion centres. In our case we begin with homogenised samples, which are quenched at low temperature. We then induced the atomic redistribution by means of ageing at a fixed temperature or by heating at constant rates. In the isothermal case the samples, initially in solid solution, are thrown off balance by the quenching, and prompted into a search for a new configuration equilibrium at the new temperature, where they are aged. In these conditions the solute atoms quit the solid solution generally by diffusion and begin to cluster, diminishing the free Gibbs energy of the system. The more stable the atomic configuration, the lower the Gibbs energy. The nucleation and growth process occurring from isothermal phenomena can be precisely read by electrical resistivity measurements; therefore, the isothermal electrical resistivity changes of the alloy relative to its homogenised microstructural state reflect its microstructural changes. The non-isothermal transformation incorporates the thermal effects, which accelerate the evolution rate and introduce new dynamical scattering centres. For that reason, it is necessary to minimise the dynamical temperature effects in order to know the structural contribution to the resistivity.

The common characteristic obtained from resistivity measurements that allow us to evaluate the transformation kinetic is the conversion degree or transformed fraction α. The mathematical relation between α and the measured properties is different for isothermal and non-isothermal measurements. Under isothermal conditions, α is assumed proportional to the evolution of the property measured during the time that the sample remains at temperature T, while no obvious relation exists between the electrical resistivity and α under non isothermal conditions. This difficulty can be smoothed out by considering kinetic reaction models of the Johnson-Mehl-Avrami type. In the present work, we propose a different way to obtain α from non-isothermal resistivity measurements without resorting to such models.

On the other hand, in previous works we have, by thermoelectric power (TEP), studied non-isothermal (5) and isothermal (6, 7) precipitation in a commercial 3003 alloy under different initial microstructural conditions. In the isothermal case, regardless of the initial microstructural condition, the Al_6(Fe, Mn) phase was identified close to 540°C. This formation was determined, mainly, by Mn diffusion with an apparent activation energy of (172 ± 8) kJ/mol; at lower temperatures and depending on the thermal treatment, the TEP behaviour was associated with the precipitation of the α-$Al_{12}Si$(Mn, Fe) metastable phase. While in our non-isothermal TEP study of the 3003 alloy we identified the characteristic temperatures associated with the different initial

microstructures, in the present work we determine, under both non-isothermal and isothermal conditions, the characteristics of the precipitated phases of the same alloy using ρ measurements.

2. Experimental details

The 3003 alloy used in the present work has the same origin as the one used in references (5-7); its composition, in weight percentage is 1.1 Mn, 0.67 Fe, 0.28 Si, 0.1 Cu, 0.01 Ti, 0.005 Zr, 0.004 Mg, 0.001 Cr, the remaining percentage being Al. The samples, whose geometry was adapted to the experimental techniques used, were homogenised during 24 hours at 600°C, quenched into an aqueous solution maintained at 0°C and then aged isothermally at different temperatures or heated at different heating rates. The objective sought with this thermal treatment is to follow the process of evolution, precipitation and/or dissolution of phases, ocurring at fixed ageing temperatures or at an increasing temperature with a constant heating rate.

For the resistivity study we used a Sigmatest D 2.068, which is a microprocessor-controlled conductivity device with a wide measuring range from 0.5 to 65 MS/m (1 to 112% IACS) and an absolute accuracy of ± 1% of the measured value. It permits to access to electrical resistivity values ranging from 1.54 to 200 μΩ cm. The samples used were square sheets of 20 x 20 mm^2 and 1 mm thick. All the measurements were made at 20°C, a temperature at which the main alloying elements show a very low diffusion. To guarantee the experimental reproducibility, only homogenised samples with an initial conductivity of 23.45 MS/m ± 1% were used. Each experimental run called for as many samples as temperature measurements were necessary. The samples were heated at different heating rates in a furnace controlled to ± 2°C.

3. Theoretical aspects

3.1. Kinetic theory

The kinetic equation that rules the precipitation processes is

$$\frac{d\alpha}{dt} = K(T,t)G(\alpha) \qquad [1]$$

where α is the conversion degree or transformed fraction, T the temperature, and t the elapsed time at that T. K is known as a reaction constant and G is the kinetic function. While isothermal treatments allow the temperature to remain fixed, non-isothermal treatments are carried out at varying temperatures; this variation establishes a T-t relation between the temperature and the time of transformation. Equation [1] is applicable to non-isothermal studies for homogeneous transformation process in temperature, (8). An integral form of that equation is written as

$$g(\alpha) = \int_0^{\alpha} \frac{d\alpha}{G(\alpha)} = \int_0^{t} K(T,t)dt \qquad [2]$$

The reaction constant K, for thermally activated processes, follows an Arrhenius relation,

$$K(T) = K_0 \exp\left(-\frac{Q}{RT}\right) \qquad [3]$$

where K_0 and the activation energy Q are the Arrhenius parameters characteristic of the kinetic under study. Solving the thermal integral and incorporating real integration limits, which permit to know the effects of T_0, an omission common to diverse kinetic models regularly used in the literature (9-13), we obtain

$$g(\alpha) = \int_0^{\alpha} \frac{d\alpha}{G(\alpha)} = \frac{K_0}{\beta} Te^{\frac{-Q}{RT}} \sum_{i=1}^{\infty} (-1)^{i+1} (i\,!)\left(\frac{RT}{Q}\right)^i + \frac{K_0 Q}{R\beta} C(T_0) \qquad [4]$$

where $C(T_0)$ is a constant depending on T_0.

Once the exponential integral is known, either in numerical or approximate form, we still require a reaction model that defines $G(\alpha)$ in equation [4] to relate the Arrhenius parameters with the transformed fraction. Isoconversional techniques, based on the invariability of $G(\alpha)$ at a fixed conversion degree permit us to overcome that inconvenience.

Equation [4] allows us to propose a more general iso-conversional equation than those proposed in the literature, since the exponent of T in that equation can be variable according to the convergence of the summation appearing in it and depending on T. Besides, the functional form of the constant $C(T_0)$, which is also written as a summation depending on T_0, could be incorporated to the analysis. Thus, attempting to comprise all these aspects, we propose the following generic iso-conversional equation for non-isothermal processes.

$$\ln\left(\frac{T^N}{\beta}\right) = \frac{Q}{RT} + C \qquad [5]$$

where exponent N is a parameter that would allow us to correct some effects of equación [4] not appearing explicitly in equation [5], as the effect of T_0, whose participation is not considered in kinetic models commonly used in kinetic analyses such as the Kissinger model (N = 2) [9] and the Ozawa model (N= 1) [13], both deducible from equation [5]. As the apparent activation energy for a fixed α value varies with N [8], this parameter can be considered a characteristic parameter of the kinetic process.

In the isothermal case and under isoconversional premises we write equation [2] as,

$$\ln\big(g(\alpha)\big) = \ln K_0 - \frac{Q}{RT} - \ln(t) \qquad [6]$$

Known $\alpha(T)$ and $\alpha(t)$, equations [5] and [6] permit us to determine the apparent activation energies of each process.

3.2 Evaluation of α using resistivity data

Although the electrical resistivity is often used to determine the conversion degree or transformed fraction $\alpha(t)$ (1, 4) under isothermal conditions, it has not been used for such purposes under non-isothermal conditions. For that reason there is no general mathematical relation that permits us to ascertain $\alpha(T)$ directly from the resistivity curves. By taking advantage of equation [1] and maintaining a constant heating rate β, We write:

$$\frac{d\alpha}{dt} = \frac{d\alpha}{dT}\frac{dT}{dt} = \beta\frac{d\alpha}{dT} \qquad [7]$$

Under isothermal conditions, at a fixed ageing T_A, $\alpha(T_A,t)$ can be written as

$$\alpha\big(T_A,t\big) = \frac{\rho\big(T_A,0\big) - \rho\big(T_A,t\big)}{\rho\big(T_A,0\big) - \rho\big(T_A,\infty\big)} \qquad [8]$$

where $\rho(T_A,0)$ is the electrical resistivity, measured immediately after quenching, that corresponds to the homogenised microstructural state; $\rho(T_A,\infty)$ is the resistivity value obtained after a long time at T_A, corresponding to a microstructural equilibrium at that temperature. Deriving equation [8] with respect to time and considering equation [7] we can obtain a mathematical expression of the derivative of α with respect to temperature,

$$\frac{d\alpha(T,t)}{dT} = -\frac{1}{\rho(T,0) - \rho(T,\infty)}\frac{d\rho(T,t)}{dT} \qquad [9]$$

Although equation [9] shows an interesting way to relate the variation of the transformed fraction with respect to temperature to the resistivity change with respect to time or temperature, it is important to determine under what conditions equation [9] is valid.

It is, therefore, necessary to differentiate between the isothermal time that is needed to attain an α transformation and the non-isothermal time needed to attain the same transformation. For any transformation path t – T, only the isokinetic reactions, studied by Avrami (14) under proportionality conditions between the nucleation and growth rates, and by Cahn (15) under more realistic physical conditions, permit us to validate equation [9]. It is important to note that the denominator in that equation is associated with the resistivity variation at a fixed temperature during an isothermal ageing, which is obviously different for each ageing temperature. This fact introduces an ambiguity factor into that equation.

A way to overcome this difficulty consists of regarding, independently of the experimental technique used for its evaluation, that α both in isothermal and in non-isothermal conditions, shows the same type of dependence on time in the isothermal case and on temperature in the non-isothermal case. α(t) or α(T) for a single transformation process is always a sigmoid curve varying between 0 and 1. This dependence on t, using equation [8] can be written as,

$$\alpha(t) = A + B\rho(t) \qquad [10]$$

with the isothermal conditions:

$\alpha(0) = 0$, for t = 0

$\alpha(\infty) = 1$ for t = ∞

which allows us to determine constants A and B in equation [10],

$$A = \frac{\rho(0)}{\rho(0) - \rho(\infty)}$$

$$B = -\frac{1}{\rho(0) - \rho(\infty)} \qquad [11]$$

A similar dependence of α on T, as equation [10], is proposed for non-isothermal cases,

$$\alpha(T) = C + D\rho(T) \qquad [12]$$

under non-isothermal conditions:

$\alpha(T_0) = 0$ for $T = T_0$

$\alpha(T_{SS}) = 0$ for $T = T_{SS}$

$\alpha(T_F) = 1$ for $T = T_F$

Under these conditions we introduce T_0, the temperature reached immediately after quenching, T_{SS}, the temperature where all precipitated phases return to the solid solution, and T_F, the temperature where the solid solution has precipitated completely. C and D in equation [12] would be fully defined by one of the first two conditions and the third; nevertheless, T_F cannot be easily taken out of a non-isothermal resistivity diagram. For that reason we derive equation [12] with respect to temperature, and by integration we obtain,

$$\frac{d\alpha}{dT} = D\frac{d\rho(T)}{dT}$$

$$\alpha(T) = D\int_{T_0}^{T}\left[\frac{d\rho}{dT}\right]dT \qquad [13]$$

D being defined by the total area under the curve $\frac{d\rho}{dT}$ versus T, i.e.

$$D = \int_{T_0}^{T_F}\left[\frac{d\rho}{dT}\right]dT \qquad [14]$$

This way T_F stays defined by the normalisation condition and it can be easily deduced from a non-isothermal diagram $\frac{d\rho}{dT}$ of versus T.

4. Results and Discussion

4.1. Isothermal study

Our isothermal study is conducted at 350°C, 400°C, 450°C, 500°C, and 550°C. Figure 1 shows the electrical resistivity of the

commercial AA3003 alloy as a function of the ageing time. Three different behaviours can be differentiated depending on the ageing temperature: the first at 350°C, the second at intermediate temperatures and the third at 550°C.

At 350°C, we observe resistivity fluctuations up to the first 3000 minutes of ageing, dropping monotonically afterwards until it reaches an equilibrium plateau for longer ageing times. The initial resistivity fluctuations are associated with the atomic redistribution of minor alloying elements such as Si and Fe, while the significant resistivity drop corresponds to the precipitation of an equilibrium phase rich in Mn, possibly an α-$Al_{12}Si$(Mn, Fe) phase, as pointed out by some authors (6).

At intermediate ageing temperatures, *i.e.* 400°C, 450°C, and 500°C, we also observe small electrical resistivity variations at the early ageing times, which can, as in the previous case, be attributed to an atomic redistribution, followed by a monotonic decrease until a slope change occurs. A final resistivity decrease occurs afterwards until an equilibrium plateau is reached. These two significant resistivity reductions are associated, the first with the precipitation of a Si-Fe-rich metastable phase, and the second with the stable equilibrium phase Al_6(Mn,Fe).

The initial electrical resistivity fluctuations at 550°C are less evident; a monotonic decrease of ρ ensues until the final plateau corresponding to the equilibrium phase Al_6(Mn,Fe) is reached.

For all heat treatments the final resistivity plateau is more prominent at lower temperatures and it is related with the greater amount of precipitable atoms, a phenomenon which is defined by the difference of atomic concentrations existing between the initial and the equilibrium concentrations at each ageing temperature. This same fact explains the behaviour of the resistivity curve

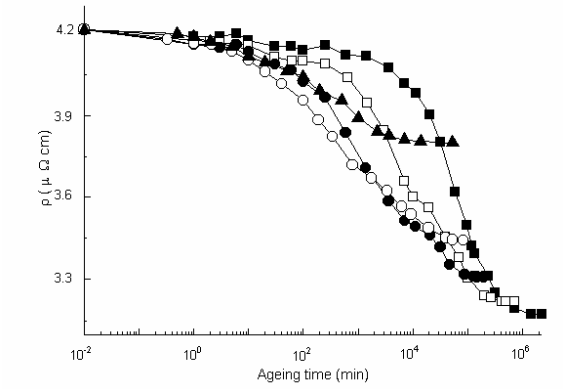

Figure 1. Isothermal electrical resistivity as a function of the ageing time for a 3003 alloy at different ageing temperatures: ■T= 350°C. □T= 400°C. ● T= 450°C ○ T= 500°C. ▲T= 550°C.

at 550°C, which seems to break the precipitation sequence shown at other temperatures. Note that although the resistivity behaviours at 350°C and 550°C appear to be similar, they correspond to the precipitation of different phases.

Using equation [8] we determine the isothermal transformed fraction α, which is shown in Figure 2 as a function of ageing time. That figure ratifies the behaviours mentioned above and makes evident the fact that a diffusive process occurs, the kinetic being faster when the ageing temperature is higher. We infer from Figures 1 and 2 that the precipitation process is associated with a decrease of the resistivity. A 2-phase precipitation is manifested at intermediate ageing temperatures of the alloy under study, in agreement with our own TEP studies (6, 7).

4.2. Non-isothermal study

Figure 3 shows the evolution of resistivity as a function of temperature for heating rates of 0.5, 1, 2, 3, 5, 10, and 20°C/min. For each case the electrical resistivity presents a slow variation at low temperatures, followed by a more pronounced fluctuation at intermediate temperatures and finally by a well defined resistivity fall with a minimum close to

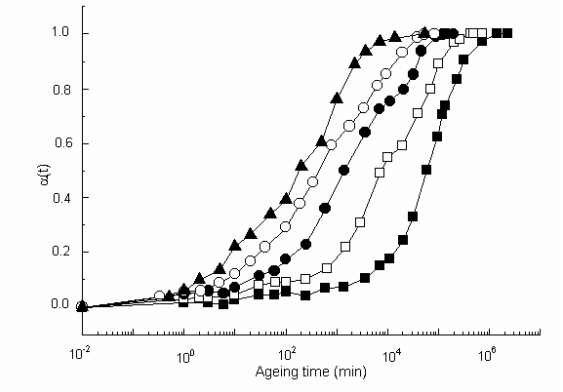

Figure 2. Isothermal precipitated fraction versus ageing time for a 3003 alloy. Same notation as in Figure 1.

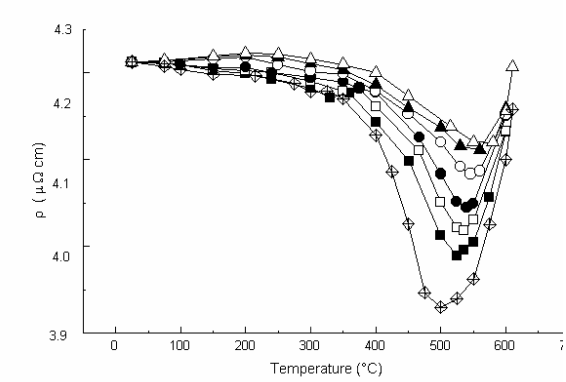

Figure 3. Non-isothermal electrical resistivity as a function of the temperature for a 3003 alloy at different heating rates in °C / min: ◈ β= 0.5. ■ β= 1. □ β= 2. ● β= 3. ○ β= 5. ▲ β = 10. △ β= 20.

500°C. Both the magnitude and the minimum position depend on the heating rate, the latter being more pronounced and located at lower temperatures when the heating rate is lower. The resistivity then increases as the precipitated phases pass into solid solution.

Again it is observed that the resistivity drop is associated with the precipitation process, while the increase of resistivity is associated with the dissolution of the precipitated phases.

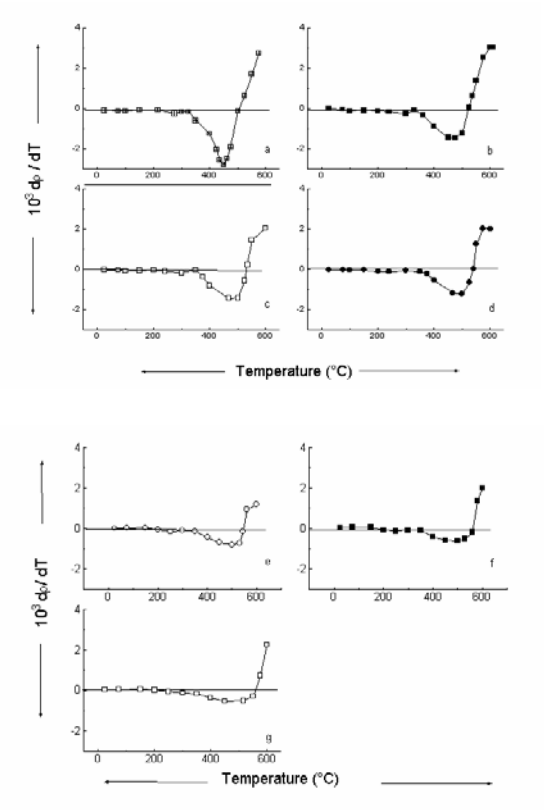

Figure 4. Derivative of the electrical resistivity with respect to temperature as a function of the temperature. a: β= 0.5°C/min. b: β= 1°C / min. c: β= 2°C / min. d: β= 3°C / min. e: β= 5°C / min. f: β= 10°C / min. g: β= 20°C / min.

Taking our previous theoretical analysis into account we proceed to obtain the derivative of the non-isothermal resistivity curves shown in Figures 4.a - 4.g. These figures have been individually drawn to focus on aspects not noticeable in the original figures. We can observe three different stages on those curves; the first, at low temperature, which, by the magnitude of the resistivity must correspond to the precipitation and dissolution of Si-rich phases; the second, better defined than the first, must correspond to the precipitation and dissolution of Fe-Si-Mn-rich metastable phases,

and the third, corresponding to the precipitation and dissolution of the Fe-Mn-rich equilibrium phase. This behaviour is in agreement with that reported in the literature (16, 17), where the equilibrium (Fe, Mn)Al_6 phase is identified near 500°C, and a group of intermediate phases of variable atomic composition are identified at lower temperatures. The best resolution in our curves corresponds to the stage of precipitation and dissolution of the equilibrium phase. We also notice that in that stage the important fall and rise of $\frac{d\rho}{dT}$ correspond to the decrease of the resistivity, which was associated to the precipitation process. Similarly, the increase in resistivity was associated with the dissolution process. For that reason the integration of equation (12) within the limits defined in that stage will furnish the transformed fraction associated with the formation of the equilibrium phase and the transformed fraction variation when such a formed phase is dissolved. Some details related to the resistivity and its derivative are summarised in Table 1 ρ_{Max} and T_ρ respectively represent the resistivity value and the temperature of the minimum of the curve versus T, while $(d\rho/dT)_{Max}$ and $T_{\rho'}$ are associated to the minimum of the curve $d\rho/dT$ versus T.

Figure 5 shows the transformed fraction associated to the equilibrium phase as a temperature function. The dissolved fraction of the precipitated phase is shown in Figure 6. Figure 5 shows that as â increases the transformed fraction tends to overlap, reason why the curve corresponding to β= 20°C/min is not included. These figures again reflect the diffusive character of the process; i.e., the displacement of α toward higher temperatures when the heating rate is greater. In Figure 6 all kinetics are made to coincide at T= 610°C where the total dissolution of the precipitated phases was expected.

4.3. Evaluation of the isothermal apparent activation energy

Using the isothermal transformed fraction shown in Figure 5 we determine the ageing time at which the same α(t) value is attained for different temperatures. In Figure 7 we draw the logarithm of the ageing time versus the temperature inverse for different α(t) values. We observe a linear dependence between the natural logarithm of the ageing time and the inverse temperature. In that figure we observe that for T = 550°C there is a linear deviation associated to the existence, at that temperature, of a phase different from the one observed at lower temperatures.

Table 1
Details of non-isothermal resistivity

β	ρ_{Max} ($\mu\Omega$ cm)	T_ρ (°C)	$(d\rho/dT)_{Max}$ ($\mu\Omega$ cm / °C)	$T\rho'$ (°C)
0.5	3.93	500	-2.79×10^{-3}	448.7
1	3.99	524.3	-1.51×10^{-3}	466
2	4.02	533.3	-1.47×10^{-3}	482.7
3	4.04	539	-1.25×10^{-3}	495.5
5	4.08	548	-0.805×10^{-3}	502.5
10	4.11	558	-0.615×10^{-3}	505
20	4.12	572	-0.555×10^{-3}	507

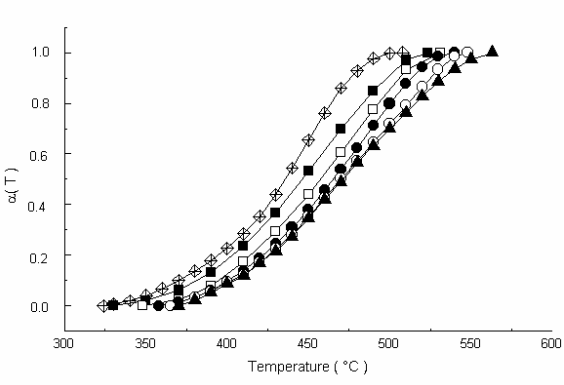

Figure 5. Non-isothermal transformed fraction versus temperature corresponding to the formation of the equilibrium phase. Same notation as Figure 3.

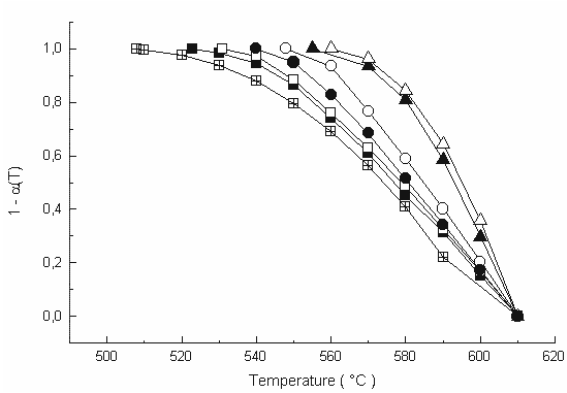

Figure 6. Non-isothermal nontransformed fraction or dissolution fraction of the equilibrium phase versus temperature Same notation as Figure 3.

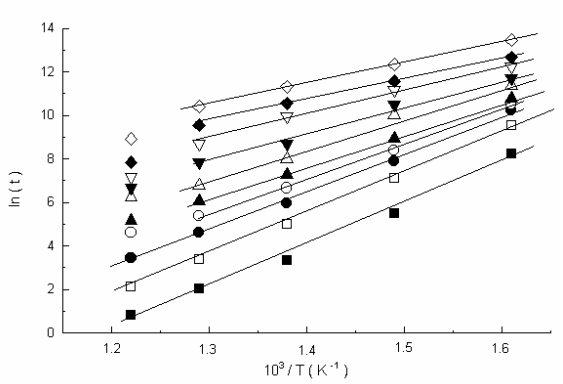

Figure 7. Natural logarithm of the ageing time versus inverse temperature for the isothermal study at different transformed fractions. ■ α= 0.1 □ α= 0.2 ●α= 0.3 ○α= 0.4 ▲α= 0.5 △ α= 0.6 ▼α= 0.7 ▽α= 0.8 ◇α= 0.9 ◇α= 0.97.

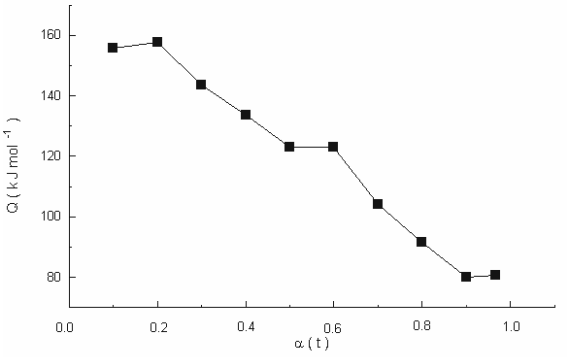

Figure 8. Apparent activation energy versus (λ) deduced from iso-conversional equation [6].

The linearity shown in Figure 7 validates the application of equation [6]. The apparent activation energy is evaluated from the slope of those straight lines. Figure 8 shows the variation of the energy versus the transformed fraction. Here we observe that Q shows a small increase for α <0.2. It then falls to a small plateau near α= 0.5 and again decreases, the energy values varying between 160 and 78 kJ/mol. Note that there are three small α ranges where the Q values remain nearly constant. These values are in agreement with those reported by Goel et al. [18], namely, 172 kJ/mol for the precipitation of Al_6Mn in an Al-1% Mn binary alloy and 141 kJ/mol for the equilibrium phase of the Al-1%Mn-0.06% Fe alloy. Decreasing the activation energy with α is associated with the incorporation of Fe atoms in the process, prompting the diffusion to take place much faster.

4.4. Evaluation of the non-isothermal apparent activation energy

The determination of the apparent activation energy of non-isothermal studies is based on equation [5] and on Figures 5 and 6 pertaining to the formation and dissolution of the equilibrium phase. Figure 9 corresponds to the phase formation stage. We show the behaviour of the natural logarithm of T^N/β versus the inverse temperature for different β heating rates. The graph corresponds to N = 2 for α = 0.1, 0.5 and 0.8. The dependence predicted by the Kissinger relation is also included in Figure 10. Independently of the α values, different slopes are observed for the lowest and highest β values, including the Kissinger case. Taking account of the overlapping of α occurring for larger β values, our next analysis will refer to the β values of 0.5, 1, 2 and 3°C/min. In Figure 10 we plot the variation of the non-isothermal apparent activation energy as a function of the N parameter for α values 0.1, 0.5 and 0.8. A linear dependence between Q and N is obtained from that curve, as observed in equation [5], the larger Q values corresponding to the lower N values. Figure 11 shows how Q varies with the transformed fraction for N = 2, 10, and 30. The phenomenological character of the N parameter is made evident, generating for N>10 activation energy values in agreement with those obtained in the isothermal study. It is important to notice that if the traditional evaluation for N = 0 and N = 2 had been used, no reproducibility of isothermal or previous (6, 7) results of energy values would have been obtained. Figure 11 also shows the activation energy evaluated from the Kissinger relation using the maximal temperature $T_{g,}$ as shown in Table 1. The Kissinger activation energy of (166 ± 5) kJ/mol obtained for the precipitation of the equilibrium phase is in agreement with the one reported by Luiggi [5] for the same Al_6(Mn,Fe) phase at (172 ± 8) kJ/mol and by Goel et al. (19) for the Al_6Mn equilibrium phase. An important fact worth mentioning is that the activation energy for the diffusion of manganese in aluminium

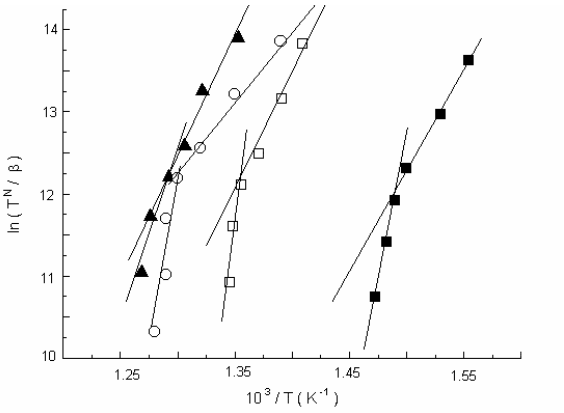

Figure 9. Natural logarithm of $\frac{T^N}{\beta}$ versus the inverse temperature for different transformed fractions of the equilibrium phase precipitation. The N parameter is fixed at 2. ■ α= 0.1 □ α= 0.5 ▲ α= 0.8 ○ Kissinger Eq.

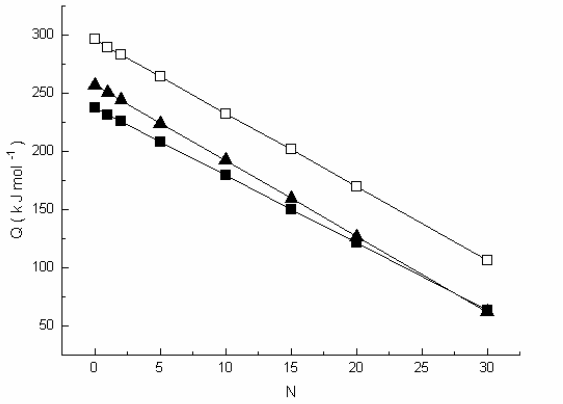

Figure 10. Apparent activation energy for the formation of the equilibrium phase versus the N parameter. ■α= 0.1 □α= 0.5 ▲α= 0.8.

amounts to (219 ± 10) kJ/mol (18) and the incorporation of alloying elements as Fe and Si diminish that activation energy, Q being higher for a fixed α when N is lower, by which we then could establish a relation between N and the quality of the alloy.

The dissolution of that phase is dealt with in Figures 12 to 14. Figure 12 shows the

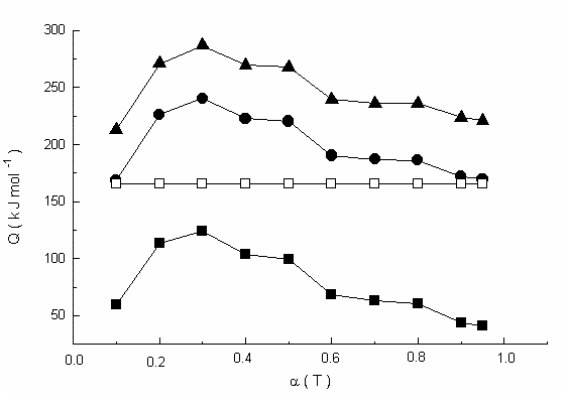

Figure 11. Apparent activation energy for the formation of the equilibrium phase versus α(T) for different N values. ▲N= 2 ●N= 10 ■N= 30. □ Energy deduced from the Kissinger Eq.

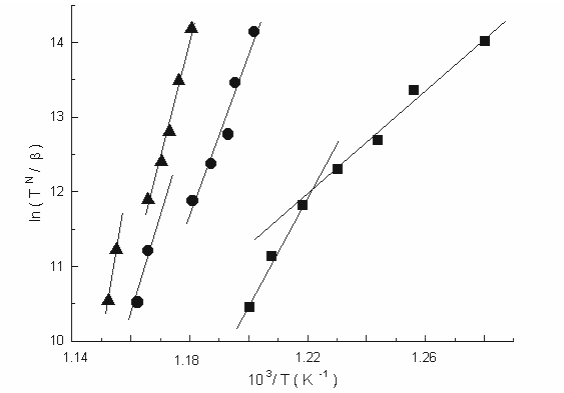

Figure 13. Apparent activation energy for the dissolution of the equilibrium phase versus N for different α(T) values. ▲α= 0.5 ●α= 0.7 ■α= 1.

behaviour of equation [5], where we plot the natural logarithm of T^N/β versus T^N, for N= 2 and α= 0.5, 0.7, and 1. Again, different behaviours are shown for the lowest and highest β values. As in the previous case, and because of the overlapping tendency of α towards higher β values, we will only consider the β values of 0.5, 1, 2, 3, and 5°C/min. The consideration of the full dissolution at 610°C, for all β values, introduces uncertainty in the α values for α 0.2. For that reason our study

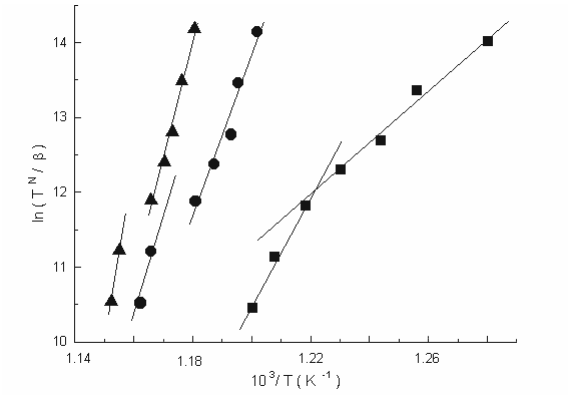

Figure 12. Natural logarithm of $\frac{T^N}{\beta}$ versus the inverse temperature for different transformed fractions during dissolution of the equilibrium phase. The N parameter is fixed at 2. ▲α= 0.5 ●α= 0.7 ■ α= 1.

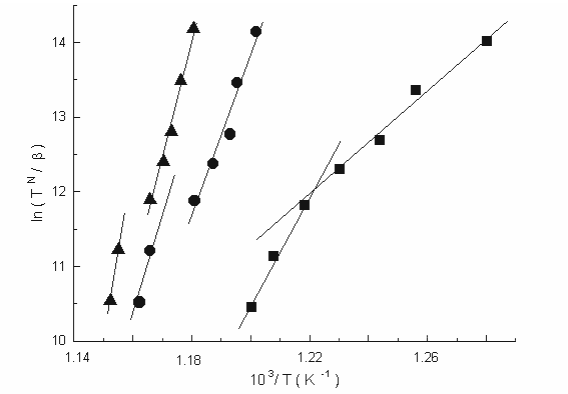

Figure 14. Apparent activation energy for the dissolution of the equilibrium phase versus α(T) for different N values. ▲N= 2 ●N= 10 ■N= 30.

will consider α values higher than 0.2. The variation of the apparent dissolution energy versus N is shown in Figure 13, for α = 0.5, 0.7, and 1. We ratify the linear relation between Q and N, the Q values being, for fixed α, lower for higher N values. Note must be taken that the Q values for the dissolution of the precipitated phase are higher than those obtained during the formation of such phase. Finally Figure 14 shows Q as a function of α.

This graph shows that as the dissolution process begins ($\alpha \approx 1$) Q reaches its minimum value (for example Q = 250 kJ/mol for N= 10), this value being larger than the Q value obtained at the end ($\alpha \approx 1$) of the precipitation process (Q = 170 kJ/mol for N = 10). As the precipitated phase dissolves, Q grows, showing a higher value when the precipitated phase ($\alpha \rightarrow 0$) approaches full dissolution.

5. Conclusions

We have studied the isothermal and non-isothermal phase transformation kinetics of a 3003 commercial alloy by electrical resistivity, concluding the following:

1. The electrical resistivity is sensible to the precipitation and dissolution of phases occurring during isothermal and non-isothermal treatments, the precipitation process being associated with a decreasing resistivity and the dissolution process with an increasing resistivity.

2. Depending on the ageing temperature, isothermal resistivity exposes small resistivity changes at the onset of ageing followed by a monophase transformation at 350°C and 550°C and a multiphase transformation at intermediate ageing temperatures.

3. Non-isothermal resistivity at different heating rates shows the precipitation and dissolution of at least three different phases, depending on the position and magnitude of the characteristic peak of the heating rate.

4. Kinetic analyses by iso-conversional techniques allow us, in the isothermal case, to differentiate between the behaviour at 550°C and that at other temperatures. The apparent activation energy calculated varies between 160 kJ/ mol and 80 kJ/mol for α values between 0.1 and 0.97. The decrease of Q is associated with the incorporation of Fe atoms in the process, which have the virtue of accelerating the kinetic, lowering the activation energy.

5. Non-isothermal kinetics permit us to distinguish three different processes, confirmed by means of a method proposed in this study to determine α, by using the derivatives of with respect to temperature. Only the stage corresponding to the equilibrium phase Al_6(Mn, Fe) was analysed, obtaining satisfactory Q values for the formation of that phase in agreement with the literature. Iso-conversional studies establish that the N parameter can be considered as a characteristic one, N being related with the alloy quality. The dissolution of Al_6(Mn,Fe) phase requires an activation energy higher than the one used in the formation stage.

Acknowledgments

This work is supported by the Consejo de Investigación de la Universidad de Oriente, under project No CI. 5-1002-0938/00 UDO, and by CONICIT under project S1- 95000844. I also want to acknowledge my appreciation to Carlos Mota and his company Traduce, C.A. for the review of this manuscript.

References

1. LUIGG N., SIMON J.P., GUYOT P. ***Acta Met*** 28: 1115-1123, 1980.
2. DOPPLER T., PFEILER W. ***J Mat Sci*** 26: 2533-2542, 1991.
3. NAGAHAMA K., MIKI I. ***Trans JIM*** 15: 185-192, 1974.
4. MÓRICZ I., SZABÓ I.A., HORDÓS M., BEKE D.L., KEDVES F. ***J Eng Materials*** 45: 265-270, 1990.
5. LUIGGI N.Z. ***Metallkd*** 274, (88): 274-277, 1997.
6. LUIGGI N. ***Metall Mater Trans*** B 28B: 125-133, 1997.
7. LUIGGI N. ***Metall Mater Trans*** B 28B: 149-159, 1997.
8. HENDERSON D.W. ***J Non-Crystalline Solids*** 30: 301-315, 1979.
9. KISSINGER H.E. ***J Res Nat Bur Stand*** 57: 217-221, 1956.

10. AUGIS J A., BENNETT, J.E. ***J Thermal Anal*** 13: 283-292, 1978.
11. COATS A.W., REDFERN, J.P. ***Nature*** 201: 68-69, 1964.
12. SATAVA V. ***Thermochim Acta*** 2: 423-428, 1971.
13. OZAWA T. ***Bull Chem Soc Japan*** 38: 1881-1886, 1965.
14. AVRAMI M. ***J Chem Phys*** 7: 1103-1112, 1939.
15. CAHN J.W. ***Acta Metall*** 4: 449-459, 1956.
16. WATANABE H., OHORI K., TAKEOUCHI Y. ***Aluminium*** 60: E310-13, 1984.
17. KOVÁCS-CSETÉNYI E., GRIGER A., TURMMEZEY T., SUCHANEK V. ***Eng Mater*** 44 (45): 271-84, 1990.
18. GOEL D.B., FURRER P., WARLIMONT. ***Aluminium*** 50: 511-516, 1974.